Science of the Total Environment 488–489 (2014) 280–289

Contents lists available at ScienceDirect

Science of the Total Environment

journal homepage: www.elsevier.com/locate/scitotenv

# Long-term trends in alkalinity in large rivers of the conterminous US in relation to acidification, agriculture, and hydrologic modification

E.G. Stets [a,*], V.J. Kelly [b], C.G. Crawford [c]

[a] National Research Program, U.S Geological Survey, 3215 Marine Street, Ste. E-127, Boulder, CO 80303, United States
[b] Oregon Water Science Center, U.S. Geological Survey, 2130 SW 5th Avenue, Portland, OR 97201, United States
[c] Indiana Water Science Center, U.S. Geological Survey, 5957 Lakeside Blvd., Indianapolis, IN 46278, United States

## HIGHLIGHTS

- We analyzed long-term trends in alkalinity and other solutes in large U.S. rivers.
- Increasing alkalinity concentration and flux were widespread.
- Considering multiple solutes provided insight into controls on alkalinity trends.
- Receding acidification and agricultural lime were linked with alkalinity increases.
- However, a diversity of processes led to alkalinity trends.

## ARTICLE INFO

*Article history:*
Received 11 March 2014
Received in revised form 14 April 2014
Accepted 14 April 2014
Available online 15 May 2014

Editor: D. Barcelo

*Keywords:*
Rivers
Trends
Alkalinity
Weathering
Acid deposition
Environmental history

## ABSTRACT

Alkalinity increases in large rivers of the conterminous US are well known, but less is understood about the processes leading to these trends as compared with headwater systems more intensively examined in conjunction with acid deposition studies. Nevertheless, large rivers are important conduits of inorganic carbon and other solutes to coastal areas and may have substantial influence on coastal calcium carbonate saturation dynamics. We examined long-term (mid-20th to early 21st century) trends in alkalinity and other weathering products in 23 rivers of the conterminous US. We used a rigorous flow-weighting technique which allowed greater focus on solute trends occurring independently of changes in flow. Increasing alkalinity concentrations and yield were widespread, occurring at 14 and 13 stations, respectively. Analysis of trends in other weathering products suggested that the causes of alkalinity trends were diverse, but at many stations alkalinity increases coincided with decreasing nitrate + sulfate and decreasing cation:alkalinity ratios, which is consistent with recovery from acidification. A positive correlation between the Sen–Thiel slopes of alkalinity increases and agricultural lime usage indicated that agricultural lime contributed to increasing solute concentration in some areas. However, several stations including the Altamaha, Upper Mississippi, and San Joaquin Rivers exhibited solute trends, such as increasing cation:alkalinity ratios and increasing nitrate + sulfate, more consistent with increasing acidity, emphasizing that multiple processes affect alkalinity trends in large rivers. This study was unique in its examination of alkalinity trends in large rivers covering a wide range of climate and land use types, but more detailed analyses will help to better elucidate temporal changes to river solutes and especially the effects they may have on coastal calcium carbonate saturation state.

Published by Elsevier B.V.

## 1. Introduction

River carbon (C) fluxes are an important link between terrestrial and marine carbon cycles (Aufdenkampe et al., 2011). Globally, rivers deliver 0.3 to 0.6 Pg C $yr^{-1}$ to oceans (Meybeck, 1993), and >75% of carbon export from the conterminous US occurs as inorganic carbon (IC; Stets and Striegl, 2012). Alterations of IC delivery can occur due to changes in chemical weathering (Amiotte Suchet et al., 1995). Surface water acidification caused by intensive agricultural production, atmospheric deposition, acid mine drainage, industrial effluents, and municipal wastewater can alter pH and carbonate buffering conditions (Meybeck, 2003) and affect fluvial IC cycling. Positive trends in alkalinity and pH since the early 1990s are common in small headwater systems and indicate a recovery from acidification (Chen and Lin, 2009; Stoddard et al., 1998, 1999). Large rivers also exhibit positive trends in alkalinity concentration and flux, but less is known about the processes driving these trends.

* Corresponding author. Tel.: +1 303 541 3048; fax: +1 303 541 3084.
*E-mail address:* estets@usgs.gov (E.G. Stets).

http://dx.doi.org/10.1016/j.scitotenv.2014.04.054
0048-9697/Published by Elsevier B.V.

Large rivers tend to have greater buffering capacity than small headwater catchments and so they are less susceptible to direct ecological effects of acidification (Johnson, 1979). Therefore, studies of acidification have mostly focused on highly susceptible headwater catchments. Nevertheless, acidic inputs interact with the carbonate buffering system and have consequences for IC biogeochemistry of large rivers. Changes in the carbonate buffering characteristics of rivers can affect coastal calcium carbonate equilibria (Duarte et al., 2013), with particularly acute effects on coastal shell-bearing organisms (Salisbury et al., 2008). Therefore, it is important to properly describe and attribute alkalinity trends in large rivers.

Increasing alkalinity flux from the Mississippi River results primarily from increased runoff (Raymond et al., 2008) whereas increasing concentrations in the Eastern U.S. are related to patterns in atmospheric deposition and recovery from acid mine drainage (Kaushal et al., 2013; Raymond and Oh, 2009). In some systems agricultural lime is important to fluvial inorganic carbon cycling (Aquilina et al., 2012; Barnes and Raymond, 2009; Hamilton et al., 2007; Oh and Raymond, 2006) although its overall significance to large rivers is not well quantified.

River alkalinity concentrations respond to a variety of factors which makes discerning the cause of alkalinity trends difficult. Increasing alkalinity can indicate recovery from acidification (Chen and Lin, 2009; Stoddard et al., 1998, 1999) because deposition of N + S acids in poorly buffered systems (alkalinity <200 μeq $L^{-1}$; Stoddard et al., 1999) consumes alkalinity and so a relaxation of this process results in positive alkalinity trends. The underlying theory of soil acidification predicts that in watersheds with ample buffering capacity accelerated weathering rates from additions of N + S acids can increase base cation and alkalinity export (Amiotte Suchet et al., 1995; Van Breemen et al., 1983). According to this theory, acidification would lead to increased alkalinity concentration and flux whereas decreased acidification would result in lower alkalinity in surface waters. However, empirical studies indicate that recovery from acidification can result in increased alkalinity even in highly buffered surface waters (Chen and Lin, 2009; Majer et al., 2005). Urbanization and changing agricultural management practices can also result in changing alkalinity in surface waters.

Urban areas have many possible sources of increased alkalinity. Concrete structures provide additional weatherable material to urban areas; weathering rates increase in disturbed soils; and, elevated $CO_2$ concentrations in aquifers receiving sewer or septic system effluent may also increase weathering rates (Barnes and Raymond, 2009). Agricultural contribution to increased alkalinity in surface waters can result from similar processes, especially the addition of agricultural lime. Agricultural liming adds carbonate minerals to soils as a means of counteracting the acidifying effects of tilling, fertilizer usage, and nitrogen-fixing plants (Hamilton et al., 2007). Addition of agricultural lime, most commonly as calcium carbonate ($CaCO_3$) or dolomite ($MgCa(CO_3)_2$), counteracts acidification by adding base cations and acid-neutralizing capacity to soils. Reactions between soil acids and agricultural lime are identical to typical carbonate weathering reactions (Table S1) and produce soluble weathering products which can affect solute concentrations in soils and nearby surface waters (Aquilina et al., 2012; Barnes and Raymond, 2009; Hamilton et al., 2007; Oh and Raymond, 2006; Perrin et al., 2008). In silicate-dominated crystalline basins, agricultural lime can be a major component of the overall IC budget (Aquilina et al., 2012).

In this study we examined alkalinity trends in large rivers of the conterminous US between the middle part of the 20th century and the early 21st century. Acidification of rivers has been expressed as a water quality concern since the early part of the 20th century (Cumming, 1916; Leitch, 1926; Purdy, 1930), mostly associated with industrial waste and acid mine drainage (AMD). Atmospheric sources of acidity increased in the middle part of the 20th century and damaged areas that were formerly pristine. Greater regulation of point sources in the U.S. has decreased direct acidic inputs to surface waters and atmospheric sulfur emissions have decreased markedly in recent decades (Smith et al., 2011). Given this context, we analyzed long-term trends in large US rivers to gain a fuller perspective on how alkalinity and other solutes have responded to the dramatic changes over that time period. We used a rigorous flow-weighting scheme to minimize the effects of changing flow regimes which allowed greater focus on changing river chemical conditions. We analyzed trends in associated ionic weathering products in order to better attribute the observed changes in alkalinity. We also use water quality data from the early 20th century to provide perspective on modern solute concentrations.

## 2. Methods

### 2.1. Ionic solute generation by chemical weathering

Chemical weathering results from the interaction of silicate or carbonate minerals with acids. Ionic weathering products are a predominant source of alkalinity and base cations to surface waters. In most soils, carbonic acid ($H_2CO_3$) produced from root and soil microbial respiration dominates chemical weathering reactions. However, N + S acids, which have both natural and anthropogenically-mediated sources, also contribute to chemical weathering (Lerman et al., 2007; Perrin et al., 2008). Nitric acid arises from nitrification of ammonium, which is a natural process that can be greatly increased by N-fertilizer additions, or from atmospheric deposition. Sulfuric acid arises from atmospheric deposition, and from pyrite oxidation, which occurs naturally but can be greatly increased by mining activity.

Increasing chemical weathering rates will increase the production of weathering products including cations, alkalinity (as $HCO_3^-$), as well as nitrate ($NO_3^-$) and sulfate ($SO_4^{2-}$) if N + S acid weathering is also increasing. Changes in the relative contribution of $H_2CO_3$ versus N + S acids will also result in trends in cation:$HCO_3^-$ ratios (Aquilina et al., 2012; Hamilton et al., 2007; Perrin et al., 2008). Reactions between $H_2CO_3$ and carbonate or silicate minerals produce cations and $HCO_3^-$ in 1:1 equivalent ratios (Table S1). When N + S acids weather carbonates in soil with circumneutral pH the reaction produces cation and $HCO_3^-$ equivalents in a 2:1 ratio (Hamilton et al., 2007), whereas the reaction between N + S acids and silicates produces no $HCO_3^-$ (Table S1; Aquilina et al., 2012). The production of $NO_3^-$ and $SO_4^{2-}$ anions instead of $HCO_3^-$ maintains charge balance. Therefore, analyzing trends in a suite of weathering products and their ratios can provide insight into the processes driving alkalinity trends.

We summarize the trend analyses included in this study and their interpretation in Table 1. As mentioned previously, alkalinity responds to a variety of pressures and so attributing a specific process to alkalinity trends is difficult. Coupling alkalinity trends with those of major cations ($Ca^{2+}$ and $Mg^{2+}$) can help to elucidate how alkalinity trends relate to overall weathering rate within the basin (Table 1). Similarly, trends in the equivalent sum of weathering-related anions, $HCO_3^- + NO_3^- + SO_4^{2-}$ ($\sum A_W$) can help indicate changes to overall weathering rates. Considering the ratio $[Ca^{2+} + Mg^{2+}]$:$HCO_3^-$ addresses how alkalinity trends relate to acidification processes (understood to mean increased weathering by N + S acids). Increasing $[Ca^{2+} + Mg^{2+}]$:$HCO_3^-$ indicates increasing prevalence of N + S acid weathering whereas a decreasing ratio indicates the opposite. A related metric, the trend in the equivalent sum of $NO_3^-$ and $SO_4^{2-}$ (N + S) can be indicative of trends acidifying processes.

### 2.2. Data sources

We assembled long-term water quality and stream discharge datasets for 23 monitoring stations selected for data availability and to represent the range of climate and land use in the conterminous US (Fig. 1, Table 2). We examined trends in alkalinity and other weathering products between the mid-20th and early 21st centuries. A separate publication describes the environmental history, geographic setting, land use changes, and data availability for most of the stations (Stets

**Table 1**
Interpretation of trend results for various metrics examined in this study.

| Metric | Positive trend | Negative trend |
|---|---|---|
| Alkalinity ($Alk_{FWC}$) | 1. Increased weathering rate.<br>2. Increased delivery of weathering products.<br>3. Recovery of soil alkalinity due to relaxation of acidification. | 1. Decreased weathering rate.<br>2. Decreased delivery of weathering products.<br>3. Depletion of soil alkalinity due to acidification processes. |
| Cations ($Ca^{2+} + Mg^{2+}$) ($[Ca^{2+} + Mg^{2+}]_{FWC}$) | 1. Increased weathering rate.<br>2. Increased delivery of weathering products. | 1. Decreased weathering rate.<br>2. Decreased delivery of weathering products.<br>3. Depletion of soil base cations. |
| $[Ca^{2+} + Mg^{2+}]:HCO_3^-$ ($[Ca^{2+} + Mg^{2+}]_{FWC}$: $Alk_{FWC}$) | 1. Increased weathering by $NO_3$ or $SO_4$ acids. | 1. Decreased weathering by $NO_3$ or $SO_4$ acids.<br>2. Recovery from acidification.<br>3. Agricultural lime additions in acidified watersheds. |
| $NO_3^- + SO_4^{2-}$ ($[N + S]_{FWC}$) | 1. Increased additions of $NO_3$ and $SO_4$ acids (i.e. through acid deposition, fertilizer usage, or natural processes). | 1. Decreased sources of $NO_3$ and $SO_4$.<br>2. Increased biological uptake of $NO_3$ or $SO_4$. |
| $HCO_3^- + NO_3 + SO_4$ ($\sum A_W$) | 1. Increased weathering rate.<br>2. Increased delivery of weathering products. | 1. Decreased weathering rate.<br>2. Decreased delivery of weathering products. |

et al., 2012). Table S2 lists several climatic variables and the level II ecoregion (Omernik, 1987) for each of the monitoring stations. We also used water quality data from the early 20th century (Clarke, 1924) to provide perspective on modern solute concentration at a subset of these monitoring stations.

### 2.3. Streamflow and water quality data

We included water quality data for the time period 1945–2010 in our analysis of yield, flow-weighted concentration, and temporal trends. None of the sites had a complete water quality record for the entire 66 year period. The number of years in a site data record ranged from 27 to 65 and averaged 50 years. In some cases, we combined water quality data from several nearby monitoring stations to create a composite water quality data record. We present a detailed list of data sources and temporal coverage in Table S3. For alkalinity we combined 18 separate parameter codes including alkalinity, acid neutralizing capacity (which was measured as an alkalinity titration), or $HCO_3^-$ (see Table S4). $HCO_3^-$ is the primary source of alkalinity in typical natural waters although borate, silicate, and organic ligands can also contribute (Hem, 1985). For the purposes of this study, we assume that $HCO_3^-$ is the dominant form of alkalinity although we discuss the potential for trends in dissolved organic carbon (DOC) to contribute to the observed alkalinity trends. We used USGS parameter codes 00915, 00925, 00945, and 00620 for $Ca^{2+}$, $Mg^{2+}$, $SO_4^{2-}$, and $NO_3^-$, respectively. We express all solutes as μeq $L^{-1}$. For trend analysis we analyzed the equivalent sum of $NO_3^-$ and $SO_4^{2-}$ (N + S). At most of the monitoring stations $SO_4^{2-}$ was much larger than $NO_3^-$ and so trends in N + S mostly reflect trends in $SO_4^{2-}$. We used USGS and US Army Corps of Engineers streamflow data (Table S3).

We also use early 20th century alkalinity, calcium, magnesium, and sulfate data in order to compare recent concentrations in these solutes with those of approximately 100 years ago. The data are from USGS Professional Paper 135 (Clarke, 1924) and are a set of samples collected at regular intervals for one water year (October–September) from the early 20th century. These samples were not appropriate for inclusion in the broader trend analysis in this paper for several reasons: 1) data were not available for all stations included in the more extensive analysis; 2) regular sampling did not resume until several decades later at most monitoring stations, making these data inappropriate for trend analysis; and, 3) daily stream discharge was often unavailable at these sites making flow-weighting impossible (see below). Therefore, we will limit the use of these samples to providing long-term perspective on modern ion concentrations at the monitoring stations of interest.

### 2.4. Load calculations and flow-weighted concentrations

We performed trend analyses on annual yields for alkalinity and on flow-weighted concentrations (FWCs) for all constituents. Trends in yield indicate changing rate of delivery over time which can occur as a result of either changing discharge or changing river chemical conditions. In contrast, FWC allows greater focus on trends in riverine chemistry occurring independently of changes in streamflow (White and Blum, 1995). We used the USGS Fortran Load Estimator program (LOADEST, Runkel et al., 2004) to calculate annual load estimates ($L_{YR}$). We developed LOADEST models in three-year segments to avoid serial correlation and to allow the concentration–discharge relationships to change over time. The results of each model were assembled chronologically to create a time series for each monitoring station. Annual yield was calculated as $L_{YR}$ divided by watershed area and expressed as meq $m^{-2}$ $yr^{-1}$. FWC was calculated as $L_{YR}$ divided by annual discharge ($Q_{YR}$) and expressed as μeq $L^{-1}$. $L_{YR}$ was output of the LOADEST routine and $Q_{YR}$ was calculated from daily stream discharge measurements. The subscript FWC is used throughout the manuscript to denote flow-weighted concentrations. For trend analysis, non-parametric statistics were used because they are robust to outliers, non-normal data distributions, and missing data. Non-parametric Kendall correlation between time (calendar year) and either annual yield or FWC was used to detect trends. The significance level was set at $P < 0.1$. The non-parametric Sen–Thiel slope was also calculated and used in a correlation analysis with land use data.

### 2.5. Ancillary data

Land use parameters used in the spatial analysis included proportion of the basin in farmland or cropland, fertilizer N usage, average lime application rate, percent of the basin in urban land use, population density, and atmospheric deposition of nitrogen and sulfur oxides. A detailed explanation of data sources and calculations for the ancillary variables appears in Stets et al. (2012); a brief explanation follows. Agricultural land use and lime application variables were calculated from the Census of Agriculture as in Broussard and Turner (2009). Farmland refers to any farm-related uses of land including pasture, row crops, orchards, fallow land, etc. Cropland is a subset of farmland and refers only to land used in row crop agriculture which is typically managed more intensively. We calculated agricultural lime usage for each basin by spatially referencing county-level Census of Agriculture data (Haines and ICPSR, 2004). The Census included a specific variable

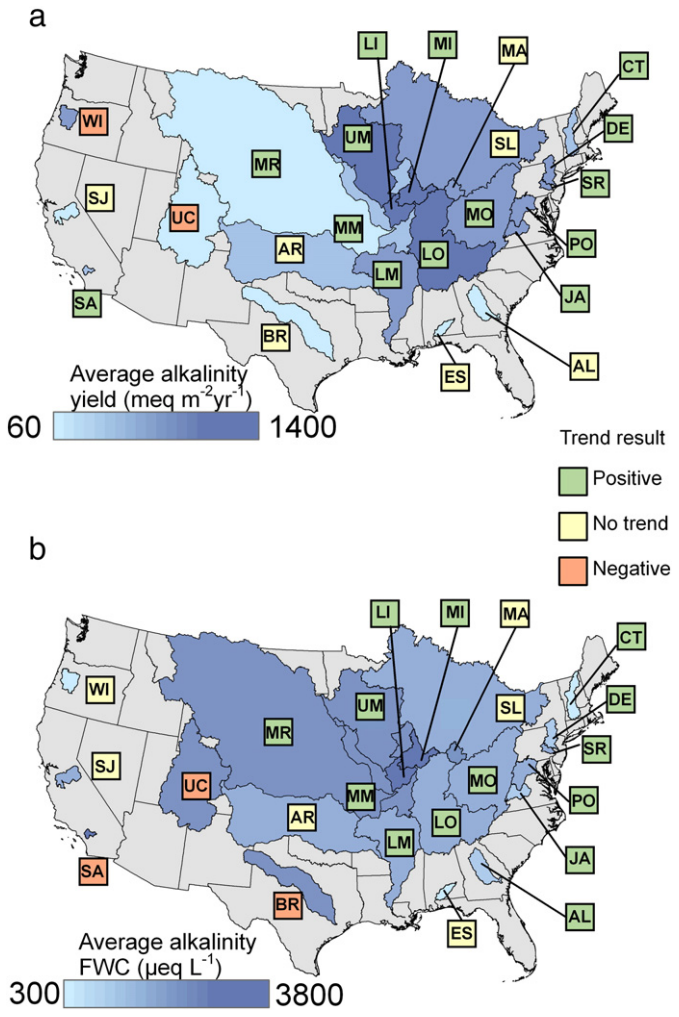


**Fig. 1.** (a) Map of alkalinity yield trend results and average (after 1997, given in meq $m^{-2}$ $yr^{-1}$) for the 23 monitoring stations included in this study. (b) Map of alkalinity flow-weighted concentration trend results and average (after 1997, given in μeq $L^{-1}$). Trend results were considered significant when $P < 0.1$ for a Kendall correlation between year annual yield or flow-weighted concentration. Monitoring station abbreviations are as follows: CT — Connecticut; DE — Delaware; SR — Schuylkill; PO — Potomac; JA — James; AL — Altamaha; ES — Escambia; MO — Middle Ohio; LO — Lower Ohio; MA — Maumee; SL — St. Lawrence; UM — Upper Mississippi; MI — Middle Illinois; LI — Lower Illinois; MR — Missouri; MM — Middle Mississippi; AR — Arkansas; LM — Lower Mississippi; BR — Brazos; UC — Upper Colorado; SA — Santa Ana; SJ — San Joaquin; WI — Willamette.

for lime usage for all census years 1952–1987, after which the Census collated lime and other amendments into a single variable. We calculated agricultural lime for all available census years and presented the average in our correlation analysis (Table S6). The proportion of the basin in farmland or cropland uses was calculated from the 2002 Census of Agriculture. Population density was calculated from county-level population data from the 2000 Decennial Population Census (http://www.census.gov/geo/maps-data/data/tiger-line.html). Urban area in each basin was calculated from the 2006 National Landcover Dataset (Fry et al., 2011). Synthetic fertilizer usage data were obtained from a published U.S. Geological Survey database (Gronberg and Spahr, 2012). County-level data were translated to river basin area by multiplying the fraction of a county in the river basin of interest by the variable of interest and then summing all of the county data across the river basin. Temporal changes in county boundaries were incorporated using the Historical U.S. County database (Earl et al., 1999).

We also examined the sum of nitrogen oxide and sulfur oxide deposition (N + S deposition) from the National Atmospheric Deposition Program (url: http://nadp.sws.uiuc.edu). We used these parameters because they are indicative of the deposition of anthropogenic acidity. For each basin, we calculated annual deposition using raster statistics. We then calculated a Sen–Thiel slope of deposition trend for each basin from 1985 to 2010 and used this in the correlation analysis (Table S5). We believe this was an appropriate metric to use for several reasons. Atmospheric N + S deposition has decreased in the US after passage of the 1990 Clean Air Act Amendments, primarily due to a decrease in S (Stoddard et al., 1999). Yet a strong spatial relationship remains between areas which had high N + S deposition prior to 1990 and those still having elevated N + S deposition. For example, a comparison of N + S deposition averaged 1985–1990 ($N + S_{Prior}$) to N + S deposition averaged 2005–2010 ($N + S_{Recent}$) for the basins included in this study demonstrates this phenomenon (Fig. S1a). A linear regression between the two produces a highly significant relationship ($N + S_{Recent} = 104 + 0.56 \times N + S_{Prior}$, $r^2 = 0.90$, $P < 0.0001$, expressed as eq $ha^{-1}$). The slope <1 indicates the extent to which N + S deposition decreased. Using average N + S deposition values to explain recent trends in riverine ionic constituents may mistakenly attribute those changes to the elevated N + S deposition occurring in these basins rather than its decrease since 1990. Similarly, a strongly negative correlation exists between the Sen Thiel slopes of N + S deposition and either $N + S_{Prior}$ or $N + S_{Recent}$ ($r = -0.93$ and $-0.78$, respectively, Fig. S1b and c). In other words, basins with the highest N + S deposition have also had the greatest reduction. Therefore, changes in riverine constituents associated with decreasing N + S deposition could be mistakenly attributed to elevated N + S deposition. This analysis is not meant to assess the 1990 Clean Air Act Amendments, but rather to find the most appropriate ways to examine the causes of alkalinity trends in large US rivers.

## 3. Results

Modern (after 1997) alkalinity yield ranged from 60 to 1392 meq $m^{-2}$ $yr^{-1}$ in the Upper Colorado and Middle Illinois Rivers, respectively (Fig. 1a). Alkalinity yield increased at 13 of the monitoring stations (Fig. 1a), mostly in the Northeastern, Midwestern, and Great Plains areas of the US (Fig. 1a). Only the Santa Ana River basin had increased alkalinity yield in the Western US (Fig. 1a). The increases were greatest in the Middle Illinois River, 557 meq $m^{-2}$ $yr^{-1}$, and averaged 138 meq $m^{-2}$ $yr^{-1}$ for all of the monitoring stations.

Trends in alkalinity yield can result either from changing chemical condition of the rivers or from increased runoff (defined as $Q_{YR}$/drainage area, m $yr^{-1}$), which enhances riverine flux of weathering products even in the absence of changes in weathering rates. Runoff increased at 8 of the 23 monitoring stations included in this study, mostly within the Upper Midwestern US (Table 3). Runoff also increased at the Middle Ohio, Lower Mississippi, and Santa Ana River monitoring stations (Table 3). Increasing runoff undoubtedly contributes to alkalinity yield in these basins over the period of analysis (Raymond and Cole, 2003). More detailed discussion of runoff trends in the Upper Midwestern US appears in several other publications (Gebert and Krug, 1996; Zhang and Schilling, 2006). In the Santa Ana River basin, runoff increases result from interbasin water transfers beginning in 1960 (Kratzer et al., 2011). Before 1965 annual runoff exceeded 0.015 m $yr^{-1}$ only in the wettest years but by the 1970s it regularly exceeded 0.020 m $yr^{-1}$ and has averaged 0.051 m $yr^{-1}$ since 1981 (not shown). We discuss runoff trends at the Santa Ana River monitoring station in greater detail below. Otherwise, consideration of runoff trends is beyond the scope of this study. Instead, we focus on trends in FWC, which are a robust indication of changes in river chemical condition (White and Blum, 1995).

$Alk_{FWC}$ (average after 1997) ranged from 313 to 3613 μeq $L^{-1}$ at the Escambia and Lower Illinois River stations, respectively (Figs. 1b and 2). $Alk_{FWC}$ increased at 14 monitoring stations, largely corresponding with alkalinity yield trends (Fig. 1a and b). Among stations with positive trends, $Alk_{FWC}$ increase averaged 292 μeq $L^{-1}$ with the largest increase at the Upper Mississippi River, 631 μeq $L^{-1}$ (Fig. 2). $Alk_{FWC}$ decreased at 3 monitoring stations, the Upper Colorado, Brazos, and Santa Ana Rivers with hydrologic modification of these basins likely contributing to

**Table 2**
Monitoring stations included in this study listed in order of USGS station ID along with their short name, latitude, and longitude. Short names are used in manuscript text.

| Monitoring station short name | Station name | Station ID | Latitude | Longitude |
|---|---|---|---|---|
| Connecticut | Connecticut River at Thompsonville, CT | 01184000 | 41°59′14″ | 72°36′19″ |
| Delaware | Delaware River at Trenton NJ | 01463500 | 40°13′18″ | 74°46′41″ |
| Schuylkill | Schuylkill River at Philadelphia, PA | 01474500 | 39°58′04″ | 75°11′19″ |
| Potomac | Potomac River (Adjusted) near Washington, DC | 01646502 | 38°56′58″ | 77°07′39″ |
| James | James River at Cartersville, VA | 02035000 | 37°40′16″ | 78°05′09″ |
| Altamaha | Altamaha River at Doctortown, GA | 02226000 | 31°39′16″ | 81°49′41″ |
| Escambia | Escambia River near Century, FL | 02375500 | 30°57′54″ | 87°14′03″ |
| Middle Ohio | Ohio River at Louisville, KY | 03294500 | 38°16′49″ | 85°47′57″ |
| Lower Ohio | Ohio River at Metropolis, IL | 03611500 | 37°08′51″ | 88°44′27″ |
| Maumee | Maumee River at Waterville OH | 04193500 | 41°30′00″ | 83°42′46″ |
| St. Lawrence | St. Lawrence River at Cornwall, Ontario near Massena, NY | 04264331 | 45°00′22″ | 74°47′42″ |
| Upper Mississippi | Mississippi River at Keokuk, IA | 05474500 | 40°23′37″ | 91°22′27″ |
| Middle Illinois | Illinois River at Kingston Mines, IL | 05568500 | 40°33′11″ | 89°46′38″ |
| Lower Illinois | Illinois River at Valley City, IL | 05586100 | 39°42′12″ | 90°38′43″ |
| Missouri | Missouri River at Hermann, MO | 06934500 | 38°42′35″ | 91°26′19″ |
| Middle Mississippi | Mississippi River at Thebes, IL | 07022000 | 37°12′59″ | 89°28′03″ |
| Arkansas | Arkansas River at Murray Dam near Little Rock, AR | 07263450 | 34°47′35″ | 92°21′30″ |
| Lower Mississippi | Mississippi River at Baton Rouge, LA | 07374000 | 30°26′44″ | 91°11′30″ |
| Brazos | Brazos River at Richmond, TX | 08114000 | 29°34′57″ | 95°45′28″ |
| Upper Colorado | Colorado River at Lees Ferry, AZ | 09380000 | 36°51′53″ | 111°35′18″ |
| Santa Ana | Santa Ana River Below Prado Dam, CA | 11074000 | 33°53′00″ | 117°38′43″ |
| San Joaquin | San Joaquin River near Vernalis, CA | 11303500 | 37°40′34″ | 121°15′59″ |
| Willamette | Willamette River at Salem, OR | 14191000 | 44°56′39″ | 123°02′34″ |

this finding. In the Colorado River the construction of the Glen Canyon Dam likely led to the retention of inorganic carbon in its reservoir, Lake Powell, which we discuss in greater detail below. Interbasin water transfers to the Santa Ana River diluted solute concentrations in this formerly groundwater-dominated system (Kratzer et al., 2011), which is consistent with our observations of increasing alkalinity yield and decreasing $Alk_{FWC}$ (Fig. 1a and b).

Increases in $Alk_{FWC}$ were more common than increases in calcium flow-weighted concentration, $Ca^{2+}_{FWC}$ (Fig. 2, Table 3), although $Ca^{2+}_{FWC}$ did increase in some areas suggesting either an increase in weathering rate or the delivery of weathering products to surface waters. In many of the largest rivers including the Lower Mississippi, Arkansas, Lower Ohio, Middle Mississippi, and Missouri Rivers, we found nonsignificant or decreasing trends in $Ca^{2+}_{FWC}$, $N + S_{FWC}$, and $\sum A_W$ (Table 3) indicating that overall weathering rate has not changed significantly in these large river basins. All weathering products had decreasing trends at the Brazos, Upper Colorado, and Santa Ana River sites, which is consistent with the role of hydrologic modification on stream solute chemistry in these basins. $Ca^{2+}_{FWC}$ increased at most monitoring stations in the Eastern U.S., and at the Upper Mississippi, Lower Illinois, and Willamette Rivers (Table 3).

Between the mid-20th and the beginning of the 21st centuries, the $Ca^{2+}_{FWC}$:$Alk_{FWC}$ and $[Ca^{2+}_{FWC} + Mg^{2+}_{FWC}]$:$Alk_{FWC}$ ratios decreased at 15 and 13 monitoring stations, respectively, while increasing at 2 and 3 monitoring stations, respectively (Table 3). The prevalence of decreasing trends in $Ca^{2+}_{FWC}$:$Alk_{FWC}$ and $[Ca^{2+}_{FWC} + Mg^{2+}_{FWC}]$:$Alk_{FWC}$ ratios suggests that acidification-driven increases in alkalinity were probably not common in the study dataset. Among the stations where the ratios increased, only the Altamaha River also had increasing $Alk_{FWC}$ (Fig. 2, Table 3), which is the expected result if N + S weathering is causing alkalinity increases. $[Ca^{2+}_{FWC} + Mg^{2+}_{FWC}]$:$Alk_{FWC}$ ratios remained >1 throughout the study period at most monitoring stations (Fig. 3),

**Table 3**
Trend results for runoff and for flow-weighted concentrations of calcium ($Ca^{2+}_{FWC}$), nitrate plus sulfate ($N + S_{FWC}$), the sum of alkalinity and N + S ($\sum A_W$). Trend results for the ratio of calcium and alkalinity ($Ca^{2+}_{FWC}$:$Alk_{FWC}$) and the ratio of calcium plus magnesium to alkalinity ($[Ca^{2+} + Mg^{2+}]_{FWC}$:$Alk_{FWC}$). The Kendall correlation coefficient ($\tau$) is shown along with an indication of significance (* = $P < 0.1$, ** = $P < 0.05$, *** = $P < 0.01$).

| Monitoring station | Runoff | $Ca^{2+}_{FWC}$ | $Ca^{2+}_{FWC}$:$Alk_{FWC}$ | $[Ca^{2+} + Mg^{2+}]_{FWC}$:$Alk_{FWC}$ | $N + S_{FWC}$ | $\sum A_W$ |
|---|---|---|---|---|---|---|
| Connecticut | 0.00 | 0.01 | −0.41*** | −0.41*** | −0.73*** | −0.35*** |
| Delaware | 0.07 | 0.43*** | −0.51*** | −0.56*** | −0.45*** | 0.17** |
| Schuylkill | 0.07 | 0.17* | −0.68*** | −0.74*** | −0.66*** | −0.12 |
| Potomac | 0.06 | 0.59*** | −0.07 | −0.23** | −0.12 | 0.43*** |
| James | 0.08 | 0.23** | 0.01 | −0.01 | −0.10 | 0.16 |
| Altamaha | −0.07 | 0.27* | 0.35** | 0.51*** | 0.55*** | 0.34** |
| Escambia | 0.05 | 0.02 | 0.12 | 0.05 | 0.60*** | 0.18 |
| Middle Ohio | 0.30** | 0.35*** | −0.50*** | −0.46*** | −0.53*** | 0.00 |
| Lower Ohio | 0.14 | 0.14 | −0.36*** | −0.30*** | −0.31*** | −0.06 |
| Maumee | 0.16 | 0.00 | −0.21* | −0.09 | −0.13 | −0.11 |
| St. Lawrence | 0.06 | −0.43*** | −0.47*** | −0.40*** | −0.47*** | 0.09 |
| Upper Mississippi | 0.31** | 0.35** | −0.23* | −0.07 | 0.34** | 0.44*** |
| Middle Illinois | 0.21* | 0.07 | −0.51*** | −0.45*** | −0.35*** | 0.22* |
| Lower Illinois | 0.24* | 0.22** | −0.25** | −0.11 | −0.49*** | −0.08 |
| Missouri | 0.23* | 0.10 | −0.5*** | −0.28*** | −0.07 | 0.10 |
| Middle Mississippi | 0.21* | −0.10 | −0.27** | −0.13 | −0.27*** | −0.02 |
| Arkansas | 0.11 | −0.39*** | −0.51*** | −0.48*** | 0.01 | 0.09 |
| Lower Mississippi | 0.27** | 0.00 | −0.57*** | −0.31*** | −0.04 | 0.14 |
| Brazos | 0.15 | −0.26*** | −0.12 | −0.02 | −0.05 | −0.18* |
| Upper Colorado | −0.17* | −0.45*** | −0.32*** | −0.22*** | −0.37*** | −0.43*** |
| Santa Ana | 0.60*** | −0.45*** | −0.09 | −0.20* | −0.31*** | −0.38*** |
| San Joaquin | 0.00 | 0.15 | 0.05 | 0.18* | 0.33*** | 0.21** |
| Willamette | −0.18 | 0.38*** | 0.37*** | 0.38*** | 0.72*** | 0.08 |

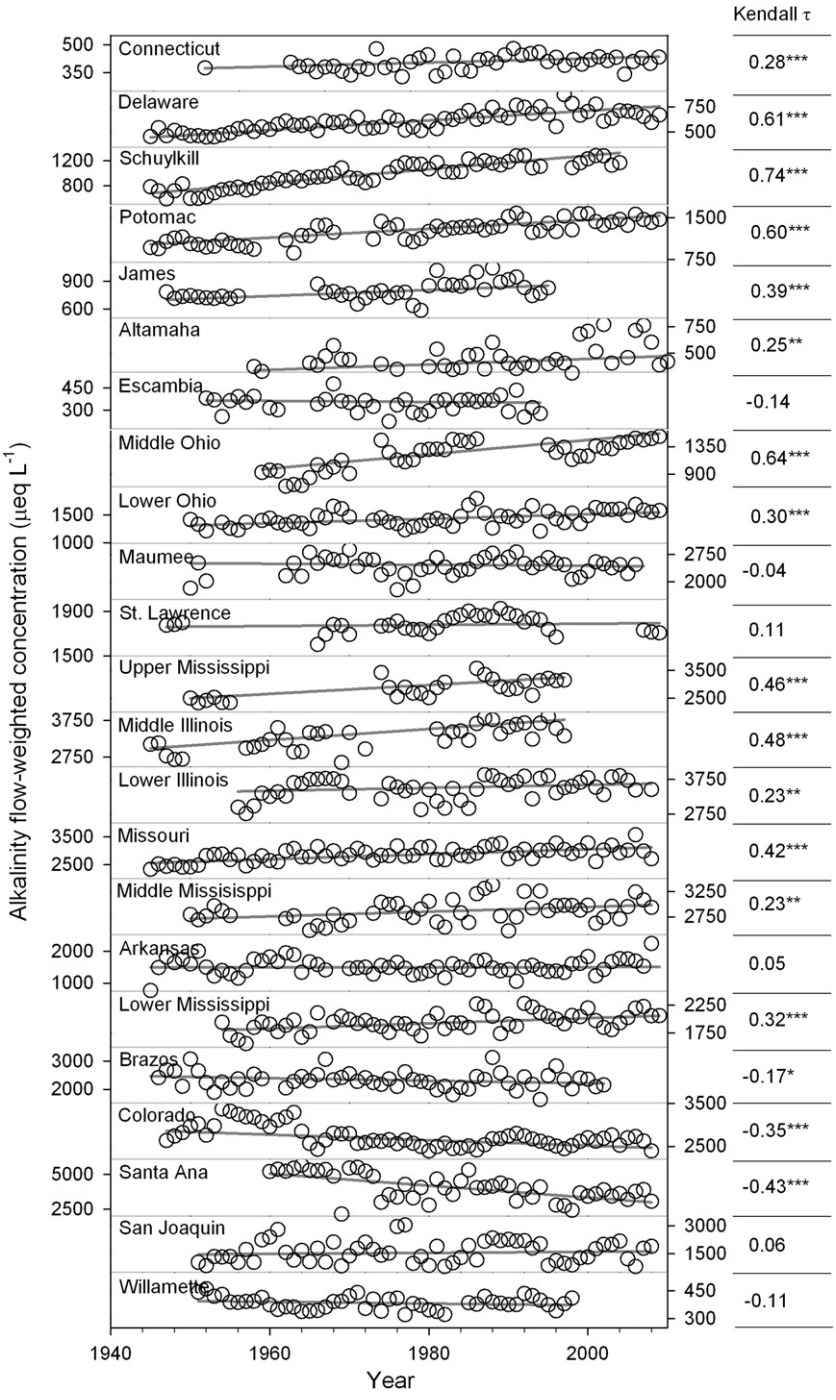


**Fig. 2.** Alkalinity annual average flow-weighted concentration, expressed in μeq $L^{-1}$, and Sen–Thiel fit for all monitoring stations along with Kendall statistic (τ). Monitoring stations are listed in ascending USGS station ID number (see Table 2). Significance level of τ is given as $^{*}P < 0.1$, $^{**}P < 0.05$, and $^{***}P < 0.01$. Note the differences in y-axis scale.

indicating that a considerable influence of N + S acid weathering remains. Ratios (averaged after 1997) were > 1.7 in the Schuylkill, Middle Ohio, and Upper Colorado Rivers, most likely due to significant weathering induced by the oxidation of sulfide-bearing minerals (Campbell et al., 1995; Raymond and Oh, 2009). Across all basins, $[Ca^{2+}_{FWC} + Mg^{2+}_{FWC}]$:$Alk_{FWC}$ averaged 1.4 and only the Willamette River site had a ratio close to 1 (Fig. 3). Nevertheless, the negative trends suggest that the role of N + S acid weathering decreased in many of the basins we studied.

We analyzed the relationships between relevant landscape parameters and the trends (Sen–Thiel slopes; Table S5) in FWC of several ionic constituents. Trends in $Alk_{FWC}$ were significantly correlated with agricultural lime usage, fertilizer usage, proportion of the basin in cropland, and population (Table 4). We also found a weakly negative correlation between $Alk_{FWC}$ trends and the Sen–Thiel slopes of N + S deposition in the basins, indicating a relation between $Alk_{FWC}$ increases and N + S deposition decreases (Table 4). Similarly, $[Ca^{2+}_{FWC} + Mg^{2+}_{FWC}]$ trends were positively correlated with agricultural lime, fertilizer usage, and proportion of the basin in cropland. These results stress the importance of agricultural processes on riverine alkalinity and cation trends. N + S trends were negatively correlated with population density and percentage of the basin in urban land uses (Table 4). This result was surprising but it may emphasize the decreasing sulfate concentrations in more populated areas associated with improvements in regulating point source pollution.

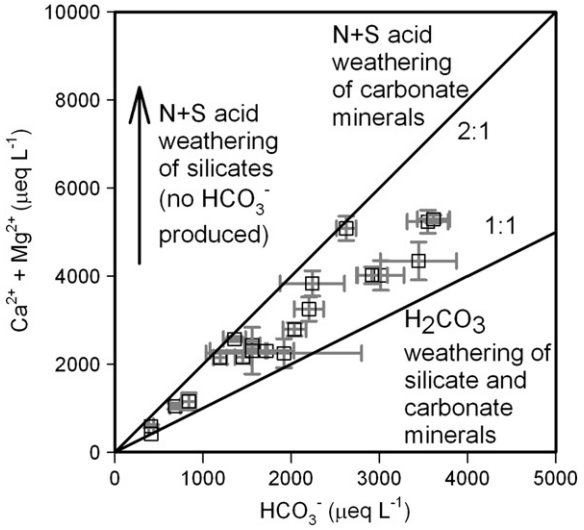


**Fig. 3.** Average (after 1997) annual flow-weighted concentration of $Ca^{2+} + Mg^{2+}$ and alkalinity, expressed as $HCO_3^-$. The 1:1 reference line is associated with weathering of carbonate and silicate minerals with $H_2CO_3$. The 2:1 reference line is associated with nitric acid and sulfuric acid (N + S acid) weathering of carbonate minerals. The arrow is associated with theoretical weathering of silicate with N + S acids which produces cations but no $HCO_3^-$.

Examining solute trends in more detail at several of the monitoring stations provided additional insight into the processes driving solute trends in this study. At the Delaware River monitoring station, increasing alkalinity largely coincided with decreases in $N + S_{FWC}$ (Fig. 4a). $Ca^{2+}_{FWC}$ increased throughout the study period, but less rapidly than $Alk_{FWC}$, which resulted in a negative trend in $Ca^{2+}_{FWC}$:$Alk_{FWC}$ ratio (Table 3). At the beginning of the time series, $N + S_{FWC}$ exceeded the range observed in the early 20th century but recent observations were more similar (Fig. 4a). $Alk_{FWC}$ increased throughout the study period, but remains below the average observed in the early 20th century (Fig. 4a). In contrast, $Ca^{2+}_{FWC}$ is higher than in the early 20th century (Fig. 4a). These results are consistent with incomplete recovery from acidification beginning in the late 20th century. Similar results were observed for the Lower Illinois River (Fig. 4b) although $Ca^{2+}_{FWC}$ greatly exceeds the range observed in the early 20th century while $Alk_{FWC}$ was similar (Fig. 4b). At the Lower Mississippi station, $N + S_{FWC}$ remains elevated compared with the early 20th century while $Alk_{FWC}$ is either similar or slightly lower than in the early 20th century (Fig. 5a). Positive trends in $Alk_{FWC}$ were not matched with positive trends in $Ca^{2+}_{FWC}$. The San Joaquin monitoring station shows great variability, but the solute trends are more consistent with intensifying acidification processes. $N + S_{FWC}$ sometimes exceeds $Alk_{FWC}$ and has been increasing over the study period (Fig. 5b, Table 3). Although we did not detect temporal trends in either $Alk_{FWC}$ or $Ca^{2+}_{FWC}$, both solutes appear to be higher in modern samples than in the early 20th century (Fig. 5b). The $[Ca^{2+}_{FWC} + Mg^{2+}_{FWC}]$:$Alk_{FWC}$ ratio also increased during the study period (Table 3).

**Table 4**
Correlation between land use parameters and the Sen–Thiel slopes of flow-weighted concentrations of alkalinity ($Alk_{FWC}$), calcium plus magnesium ($[Ca^{2+} + Mg^{2+}]_{FWC}$) and nitrate plus sulfate ($N + S_{FWC}$). The land use parameters include agricultural lime application (average 1952–1987), N fertilizer application (average 2000–2006), percent of the basin in urban land use, proportion of the basin in either farmland or cropland, population density, and the Sen–Thiel slope of atmospheric deposition of nitrogen and sulfur oxides (N + S deposition). The Kendall correlation coefficient ($\tau$) is shown. * = $P < 0.1$, ** = $P < 0.05$, *** = $P < 0.01$.

| | $Alk_{FWC}$ | $[Ca^{2+} + Mg^{2+}]_{FWC}$ | $N + S_{FWC}$ |
|---|---|---|---|
| Lime | 0.46*** | 0.36** | −0.17 |
| Fertilizer | 0.33** | 0.29* | −0.05 |
| Urban | 0.18 | 0.01 | −0.33** |
| Farmland | 0.23 | 0.20 | −0.01 |
| Cropland | 0.38** | 0.29* | −0.10 |
| Population | 0.24* | 0.09 | −0.33** |
| N + S deposition trend | −0.24* | −0.11 | 0.06 |

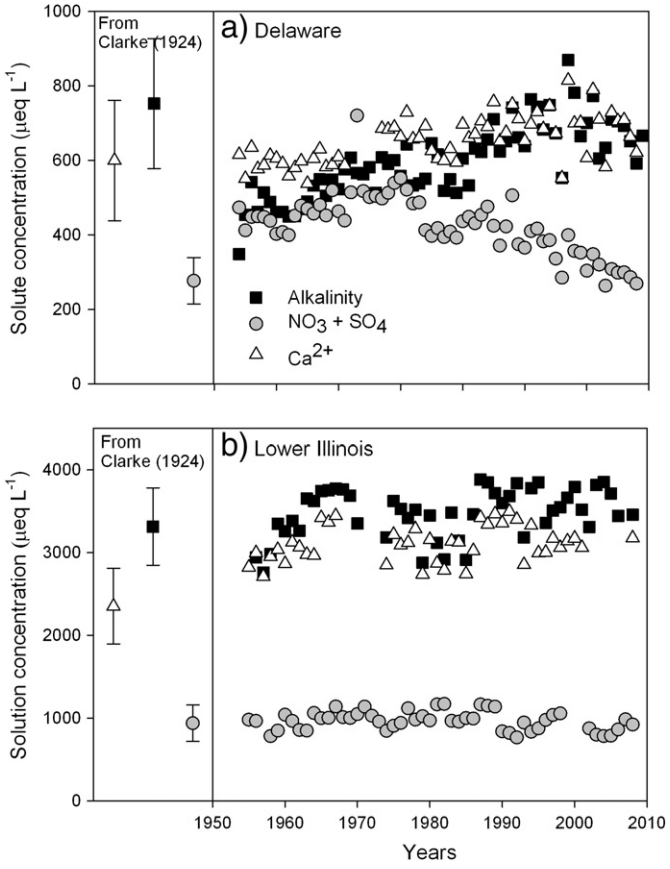


**Fig. 4.** Annual flow-weighted concentrations of alkalinity, calcium ($Ca^{2+}$) and the equivalent sum of nitrate and sulfate ($NO_3^- + SO_4^{2-}$) for the (a) Delaware and (b) Lower Illinois River monitoring stations. The average and standard deviation of concentration of each solute from the early 20th century (Clarke, 1924) are also displayed for comparison.

Despite the recent alkalinity increases noted here and in other studies, alkalinity was remarkably similar between the early 20th century observations and those made after 1997 (Fig. 6a). The Arkansas, Maumee, and Santa Ana Rivers had modern alkalinity concentrations that were lower than in the early 20th century whereas the Potomac and San Joaquin had higher modern values (Fig. 6a). In contrast, $Ca^{2+}$ and, to a greater extent, N + S had a greater tendency to be elevated in modern samples as compared with the early 20th century (Fig. 6b and c). The $[Ca^{2+} + Mg^{2+}]$:Alk ratio averaged 1.2 ± 0.2 (std. dev.) in the early 20th century as compared with 1.4 ± 0.2 for $[Ca^{2+}_{FWC} + Mg^{2+}_{FWC}]$:$Alk_{FWC}$ in observations made after 1997 (data not shown). These results are consistent with a persistent, although potentially lessening, influence of acidification processes on large rivers of the conterminous U.S.

## 4. Discussion

The alkalinity trends observed in this study were the result of a diversity of causes. Many of the sites exhibited trends consistent with long-term, although incomplete, recovery from acidification along with additional sources of weathering products to rivers, most likely in the form of agricultural lime (Table 4). The strongest evidence for acidification recovery at these monitoring stations was widespread decreases in $Ca^{2+}_{FWC}$:$Alk_{FWC}$ and $[Ca^{2+}_{FWC} + Mg^{2+}_{FWC}]$:$Alk_{FWC}$ along with decreases in $N + S_{FWC}$ (Table 3). Increasing alkalinity was also correlated with decreases in N + S atmospheric deposition (Table 4), although it is important to reiterate that large rivers have the potential to become acidified through multiple point and nonpoint sources, so recovery from

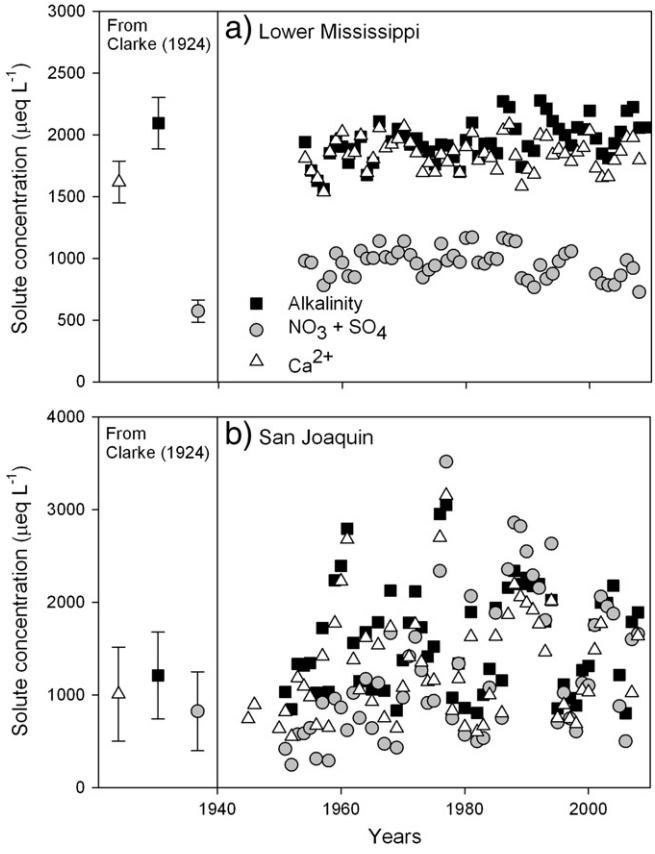


**Fig. 5.** Annual flow-weighted concentrations of alkalinity, calcium ($Ca^{2+}$) and the equivalent sum of nitrate and sulfate ($NO_3^- + SO_4^{2-}$) for the (a) Lower Mississippi and (b) San Joaquin River monitoring stations. The average and standard deviation of concentration of each solute from the early 20th century (Clarke, 1924) are also displayed for comparison.

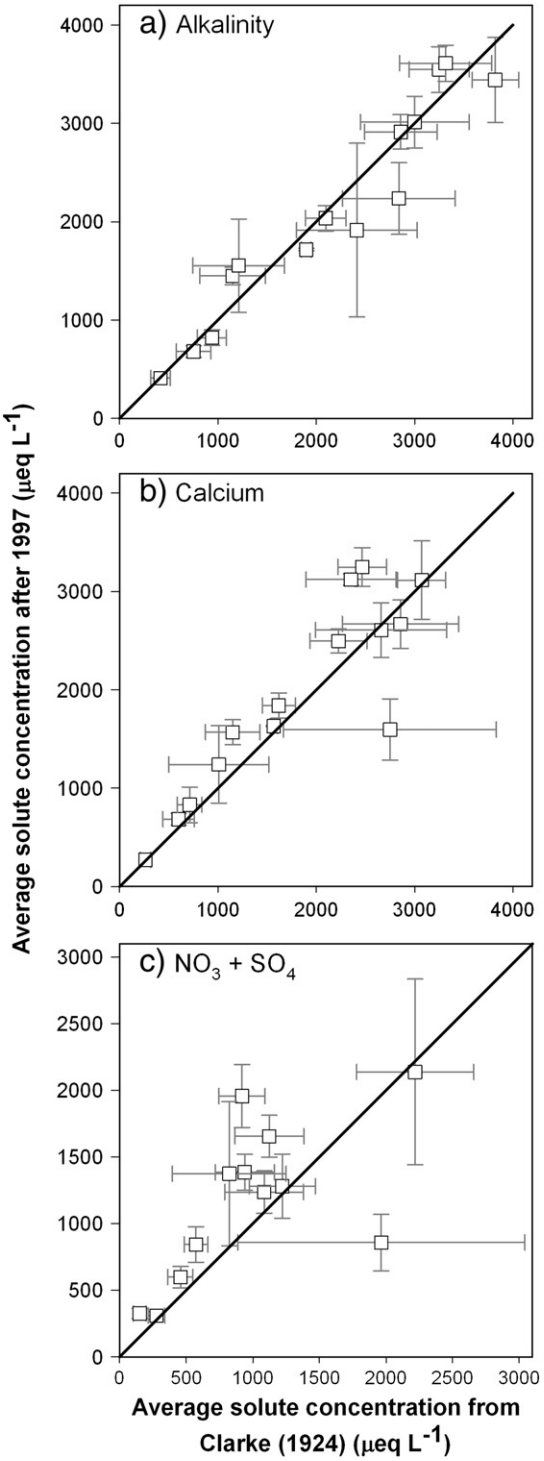


**Fig. 6.** Average concentration of (a) alkalinity (as $HCO_3^-$), (b) calcium, and (c) the equivalent sum of nitrate and sulfate ($NO_3^- + SO_4^{2-}$) from the early 20th century (Clarke, 1924) and averaged after 1997 (as flow-weighted concentrations).

acidification could indicate improvement in any of these potential sources. Acidifying processes can consume alkalinity by protonating $HCO_3^-$ to form $H_2CO_3$, which can be lost from surface waters as $CO_2$. Therefore, acidification has important consequences for riverine carbon cycling (Raymond and Oh, 2009). Likewise, increasing alkalinity occurring as a result of decreasing acidity ultimately increases DIC flux from continents to the coastal ocean and can increase aragonite saturation in coastal areas with important implications for coastal shell-bearing organisms (Salisbury et al., 2008). The finding that alkalinity increases in some areas were likely related to decreasing acidity implies that aragonite saturation state may be improving in some rivers. However, we emphasize that the rivers included in this study are geographically diverse and the solute trends defy simple explanation. The most striking counterexamples were decreases in alkalinity and other weathering products in the hydrologically modified Upper Colorado, Brazos, and Santa Ana River monitoring stations.

Decreases in concentration of weathering products in the Santa Ana River occurred due to dilution with water originating from outside of the basin whereas the decreases in the Upper Colorado and Brazos Rivers reflect retention of weathering products in reservoirs. Approximately 25% of the annual discharge from the Santa Ana River originates from northern California and the Colorado River (Kratzer et al., 2011). Historically, groundwater was the principal water source in this basin and was likely to contain higher concentrations of weathering products than interbasin water transfers. Therefore, dilution is a likely explanation for sharp declines in all weathering products observed in this study (Fig. 2, Table 3). Calcite precipitation in Lake Powell is a likely explanation for the decreasing trends in weathering products observed at the Upper Colorado station (Fig. 2, Table 3). Calcite precipitation has been documented in Lake Powell (Reynolds and Johnson, 1974) and calcite saturation indices at several stations in Lake Powell were routinely positive during the period 1964–2012 (data from Vernieu (2013), calculated using PHREEQC (Parkhurst and Appelo, 2013)). On the Brazos River, large flood control and water storage reservoirs were constructed throughout the mid-20th century (Vogl and Lopes, 2009). Calculated calcite saturation indices were always positive in three of the largest

reservoirs, Possum Kingdom Lake, Lake Whitney, and Waco Lake (USGS station ID 08088500, 08092500, and 313148097140601, respectively; url: http://waterdata.usgs.gov/nwis). Dissolved inorganic carbon (DIC) in the Brazos River originates from atmospheric invasion of $CO_2$ and dissolution of marine carbonates, rather than respiration of organic material (Zeng et al., 2010), which is consistent with the elevated pH typically associated with calcite precipitation. In these systems, hydrologic modification was likely the major factor causing solute trends.

In the Eastern US, abatement of AMD or reductions in other sources of acidity are likely to have caused increasing alkalinity in at least several of the sites. However, positive trends in $Ca^{2+}_{FWC}$ complicate this interpretation. Acid deposition can increase soil calcium mobility and lead to calcium depletion in sensitive forest soils (Huntington, 2000; Likens et al., 1998). Therefore, decreasing base cation concentrations in stream water have been interpreted as recovery from acidification (Stoddard et al., 1999). Likewise, increasing calcium and alkalinity concentrations were interpreted to indicate increasing weathering due to acidification in Eastern streams (Kaushal et al., 2013). However, our findings of decreasing $[Ca^{2+} + Mg^{2+}]_{FWC}$:$Alk_{FWC}$ and decreasing $N + S_{FWC}$ in many Eastern streams are indicative of decreasing acidity (Table 3). AMD is a widespread problem in the Eastern U.S. (Herlihy et al., 1990) and positive alkalinity trends in the Schuylkill River resulted from AMD abatement (Raymond and Oh, 2009). Similarly, serious AMD problems existed in the Potomac River basin, especially the North Branch Potomac River, in the mid-20th century but have improved in some areas (Mills and Davis 2000; Stets et al., 2012). Alkalinity increases in the Delaware River were generally coincident with decreases in $N + S_{FWC}$ (Fig. 4a), which is consistent with decreasing acidification at that monitoring station as well. So the causes of alkalinity increases in the Eastern U.S. are likely to be diverse, but at several stations, there appeared to be a link with AMD recovery or reductions in other sources of acidity. Increasing calcium in Eastern rivers is more difficult to explain in this context, but agricultural lime is a potential source of additional weathering products.

Positive correlations exist in our dataset between $Alk_{FWC}$ trends and several indicators of agricultural production including cropland area, fertilizer usage, and lime application (Table 4). Agricultural production could increase weathering rates through soil disturbance and other means of increasing soil respiration (Schlesinger and Andrews, 2000), which increase soil $CO_2$ concentration. However, the effects of agriculture on soil respiration are not clear (Raich and Tufekciogul, 2000). Agricultural lime is a prominent source of weathering products in agricultural areas. Averaged over the period 1952–1987, agricultural lime added 0 to 500 meq $m^{-2}$ $yr^{-1}$ of alkalinity to the basins included in this study (Table S6). In the Potomac, Escambia, and Altamaha Rivers, agricultural lime additions exceeded 40% of the alkalinity yield from the basin (Fig. 1a, Table S6), suggesting that a trend in alkalinity could result if even a small percentage of the lime added was delivered to surface waters as alkalinity. Agricultural lime dissolution can occur through reactions with $H_2CO_3$ or N + S acids. Because of the prevalence of reduced nitrogen additions to agricultural soils as fertilizer, manure, or by N-fixing plants, reaction with $HNO_3$ produced through nitrification is a prevalent pathway of lime dissolution (Barnes and Raymond, 2009). This reaction delivers $[Ca^{2+} + Mg^{2+}]$ and $HCO_3^-$ in a 2:1 ratio (Table S1). As a result, the $[Ca^{2+} + Mg^{2+}]$:$HCO_3^-$ ratio in agricultural streams often exceeds 1.5 (Aquilina et al., 2012; Hamilton et al., 2007; Perrin et al., 2008), underscoring the importance of N + S acid weathering in these systems. At most of the monitoring stations we examined, the $[Ca^{2+} + Mg^{2+}]$:$HCO_3^-$ ratio decreased throughout the study period (Table 3), suggesting that any increases in agriculturally-derived alkalinity may have been offset by reductions in acidity elsewhere in the basin. However, it is important to note that several of the monitoring stations exhibited trends more consistent with increasing acidity due to agricultural input or other processes.

Increasing acidification was evident at the Upper Mississippi and Altamaha monitoring stations, which had increases in $Alk_{FWC}$ (Figs. 1b and 2) along with increases in either $[Ca^{2+} + Mg^{2+}]_{FWC}$:$Alk_{FWC}$ or $N + S_{FWC}$ (Table 3). In the Altamaha River, the FWC of all weathering products increased which was consistent with enhanced weathering due to inputs of N + S acids (Figs. 1b and 2, Table 3). Dissolution of agricultural lime with N + S acids, or continuing acidification through acid deposition may explain this result (Table S6). In the Upper Mississippi, positive trends in all weathering products along with stable $[Ca^{2+} + Mg^{2+}]_{FWC}$:$Alk_{FWC}$ indicated increased weathering rates (Figs. 1b and 2, Table 3). The Upper Mississippi is one of the most purely agricultural basins in this study (Table S6). The relatively low urban coverage in the Upper Mississippi may present fewer areas where agricultural acidification could be offset by improvements in point source regulation and therefore stream solute trends reflect agriculturally-driven acidification.

At the San Joaquin River monitoring station, increasing $[Ca^{2+} + Mg^{2+}]_{FWC}$:$Alk_{FWC}$ and $N + S_{FWC}$ (Table 3) may be related to trends in return-flow irrigation water. Intensive water management in this basin results in unusually high solute concentration variability relating to water releases from reservoirs in the upper basin (Fig. 5b, Kratzer et al., 2011). In dry years irrigation diversions can exceed water supply such that water in the San Joaquin can theoretically be used several times before discharging to the San Joaquin–Sacramento delta (Kratzer et al., 2011). $NO_3$ concentrations and loads have been found to be increasing steadily in this basin (Kratzer et al., 2011). $[Ca^{2+} + Mg^{2+}]_{FWC}$:$Alk_{FWC}$ and $N + S_{FWC}$ both increased in low-runoff years (not shown) suggesting that the influence of return-flow irrigation water is a major control on solute concentrations.

Dissolved organic carbon (DOC) trends were not likely to play a role in the observed alkalinity trends in this study. DOC contribution to alkalinity is only significant in rivers with relatively low alkalinity concentrations ($<500$ μeq $L^{-1}$, Stets and Striegl, 2012). For most of the stations included in this study, $Alk_{FWC}$ was much higher and so DOC contributions to alkalinity were likely to be very low (Fig. 2). However, at several of the monitoring stations, $Alk_{FWC}$ was relatively low and had positive trends, particularly in the beginning of the study period. These included the Connecticut, Delaware, and Altamaha Rivers (Fig. 2). For these monitoring stations, we analyzed available DOC and total organic carbon (TOC) trends using Kendall correlation. The DOC and TOC records for these stations begin in the 1970s and show either no trend (Altamaha River, $\tau = -0.01$, $P = 0.72$, $n = 315$) or negative trends (Delaware River, $\tau = -0.40$, $P < 0.0001$, $n = 262$; Connecticut River, $\tau = -0.13$, $P < 0.0001$, $n = 413$). No flow-weighting or seasonal differences were considered in the DOC trend analysis, so they should be considered preliminary. But they suggest that the alkalinity increases were not caused by increasing organic ligand concentration.

## 5. Conclusions

Our analysis of long-term trends in a suite of solutes, their ratios, and accompanying land use elucidated connections between alkalinity trends and recovery from acidification, agricultural production, and hydrologic modification. As urbanization and agricultural production expand globally, it will be important to properly attribute these processes to changes in riverine carbon cycling and carbonate equilibria, especially in relation to coastal processes. The experience of improving acid conditions in some large U.S. rivers serves as an important counterexample to other areas presently undergoing rapid industrialization (Rice and Herman, 2012). In the Changjiang River basin, $H_2SO_4$ contributes substantially to chemical weathering and recent increases in $SO_4^{2-}$, attributed to acid deposition and municipal inputs suggest increasing acidification in this regionally significant river (Chetelat et al., 2008). In the Huanghe River basin, extensive dam building and agricultural diversions have led to preferential alkalinity consumption, an acidifying reaction, and progressively higher $[Ca^{2+} + Mg^{2+}]$:$HCO_3^-$ (Chen et al., 2005). These trends could have significant effects on coastal acidification by reducing alkalinity export to coastal areas.

## Acknowledgments

This work was funded as part of the USGS National Water Quality Assessment Century of Trends project. We thank Gretchen Oelsner and Pete Murdoch, who reviewed earlier versions of this manuscript. E.G.S, V.J.K, and C.G.C have no conflicts of interest to declare.

## Appendix A. Supplementary data

Supplementary data to this article can be found online at http://dx.doi.org/10.1016/j.scitotenv.2014.04.054.

## References

Amiotte Suchet P, Probst A, Probst JL. Influence of acid rain on $CO_2$ consumption by rock weathering: local and global scales. Water Air Soil Pollut 1995;85:1563–8. http://dx.doi.org/10.1007/BF00477203.

Aquilina L, Poszwa A, Walter C, Vergnaud V, Pierson-Wickmann A-C, Ruiz L. Long-term effects of high nitrogen loads on cation and carbon riverine export in agricultural catchments. Environ Sci Technol 2012;46:9447–55. http://dx.doi.org/10.1021/es301715t.

Aufdenkampe AK, Mayorga E, Raymond PA, Melack JM, Doney SC, Alin SR, et al. Riverine coupling of biogeochemical cycles between land, oceans, and atmosphere. Front Ecol Environ 2011;9:53–60. http://dx.doi.org/10.1890/100014.

Barnes RT, Raymond PA. The contribution of agricultural and urban activities to inorganic carbon fluxes within temperate watersheds. Chem Geol 2009;266:318–27. http://dx.doi.org/10.1016/j.chemgeo.2009.06.018.

Broussard W, Turner RE. A century of changing land-use and water-quality relationships in the continental US. Front Ecol Environ 2009;7:302–7. http://dx.doi.org/10.1890/080085.

Campbell DH, Clow DW, Ingersoll GP, Mast MA, Spahr NE, Turk JT. Processes controlling the chemistry of two snowmelt-dominated streams in the Rocky Mountains. Water Resour Res 1995;31:2811–21. http://dx.doi.org/10.1029/95WR02037.

Chen Y, Lin L-S. Responses of streams in central Appalachian Mountain region to reduced acidic deposition—comparisons with other regions in North America and Europe. Sci Total Environ 2009;407:2285–95. http://dx.doi.org/10.1016/j.scitotenv.2008.11.035.

Chen J, Wang F, Meybeck M, He D, Xia X, Zhang L. Spatial and temporal analysis of water chemistry records (1958–2000) in the Huanghe (Yellow River) basin. Global Biogeochem Cycles 2005;19:GB3016. http://dx.doi.org/10.1029/2004GB002325.

Chetelat B, Liu CQ, Zhao ZQ, Wang QL, Li SL, Li J, et al. Geochemistry of the dissolved load of the Changjiang Basin rivers: anthropogenic impacts and chemical weathering. Geochim Cosmochim Acta 2008;72:4254–77. http://dx.doi.org/10.1016/jgca.2008.06.013.

Clarke FW. The composition of the river and lake waters of the United States. US Geol Surv Prof Pap 1924;135:205.

Cumming HS. Investigation of the pollution and sanitary conditions of the Potomac watershed. US Public Health Serv Hygenic Lab Bull 1916;104:283.

Duarte CM, Hendriks IE, Moore TS, Olsen YS, Steckbauer A, Ramajo L, et al. Is ocean acidification an open-ocean syndrome? Understanding anthropogenic impacts on seawater pH. Estuar Coasts 2013;36:221–36. http://dx.doi.org/10.1007/s12237-013-9594-3.

Earl C, Otterstrom S, Heppen J. HUSCO 1970–1999: historical United States county boundary files. Geosciences publications. Baton Rouge, LA: Department of Geography and Anthropology, Louisiana State University; 1999.

Fry J, Xian G, Jin S, Dewitz J, Homer C, Yang L, et al. Completion of the 2006 national land cover database for the conterminous United States. Photogramm Eng Remote Sens 2011;77:858–64.

Gebert WA, Krug WR. Streamflow trends in Wisconsin's driftless area. J Am Water Resour Assoc 1996;32:733–44. http://dx.doi.org/10.1111/j.1752-1688.1996.tb03470.x.

Gronberg JM, Spahr NE. County-level estimates of nitrogen and phosphorus from commercial fertilizer for the conterminous United States, 1987–2006. U.S. Geological Survey scientific investigations report 2012–5207; 2012. p. 20.

Haines MR, Inter-university Consortium for Political and Social Research (ICPSR). Historical, demographic, economic, and social data: the United States, 1790–2000, dataset 2896, Ann Arbor, MI; 2004.

Hamilton SK, Kurzman AL, Arango C, Jin L, Robertson GP. Evidence for carbon sequestration by agricultural liming. Global Biogeochem Cycles 2007;21:GB2021. http://dx.doi.org/10.1029/2006GB002738.

Hem JD. Study and interpretation of the chemical characteristics of natural water. U.S. Geological Survey water supply paper 2254; 1985. p. 264.

Herlihy AT, Kaugmann PR, Mitch ME. Regional estimates of acid mine drainage impact on streams in the mid-Atlantic and Southeastern United States. Water Air Soil Pollut 1990;59:91–107. http://dx.doi.org/10.1007/BF00284786.

Huntington TG. The potential for calcium depletion in forest ecosystems of southeastern United States: review and analysis. Global Biogeochem Cycles 2000;14:623–38. http://dx.doi.org/10.1029/1999GB001193.

Johnson NM. Acid rain: neutralization within the Hubbard Brook ecosystem and regional implications. Science 1979;204:497–9. http://dx.doi.org/10.2307/1748806.

Kaushal SS, Likens GE, Utz RM, Pace ML, Grese M, Yepsen M. Increased river alkalinization in the Eastern U.S. Environ Sci Technol 2013;47:10302–11. http://dx.doi.org/10.1021/es401046s.

Kratzer CR, Kent RH, Seleh DK, Knifong DL, Dileanis PD, Orlando JL. Trends in nutrient concentrations, loads, and yields in streams in the Sacramento, San Joaquin, and Santa Ana Basins, California, 1975–2004. US Geol Surv Sci Investig Rep 2011:112.

Leitch RD. Stream pollution by acid mine drainage. U.S. Bureau of Mines report of investigations; 1926. p. 2725. [Washington DC].

Lerman A, Wu L, Mackenzie FT. $CO_2$ and $H_2SO_4$ consumption in weathering and material transport to the ocean, and their role in the global carbon balance. Mar Chem 2007;106:326–50. http://dx.doi.org/10.1016/j.marchem.2006.04.004.

Likens GE, Driscoll CT, Buso DC, Siccama TG, Johnson CE, Lovett GM, et al. The biogeochemistry of calcium at Hubbard Brook. Biogeochemistry 1998;41:89–173. http://dx.doi.org/10.1023/A:1005984620681.

Majer V, Krám P, Shanley JB. Rapid regional recovery from sulfate and nitrate pollution in streams of the western Czech Republic — comparison to other recovering areas. Environ Pollut 2005;135:17–28. http://dx.doi.org/10.1016/j.envpol.2004.10.009.

Meybeck M. Riverine transport of atmospheric carbon: sources, global typology and budget. Water Air Soil Pollut 1993;70:443–63. http://dx.doi.org/10.1007/BF01105015.

Meybeck M. Global analysis of river systems: from Earth system controls to Anthropocene syndromes. Philos Trans R Soc Lond B Biol Sci 2003;358:1935–55. http://dx.doi.org/10.1098/rstb.2003.1379.

Mills JE, Davis TL. The recovery of the North Branch - 1940 to 2000 and beyond. Maryland Department of the Environment. Frostburg MD: Bureau of Mines, Frostburg State University; 2000. p. 11.

Oh N-H, Raymond PA. Contribution of agricultural liming to riverine bicarbonate export and $CO_2$ sequestration in the Ohio River basin. Global Biogeochem Cycles 2006;20:GB3012. http://dx.doi.org/10.1029/2005GB002565.

Omernik JM. Ecoregions of the conterminous United Stets. Map (scale 1:7,500,000). Annals of the Association of American Geographers 1987; 77: 118–125, doi: 10.1111/j.1467-8306.1987.tb00149.x.

Parkhurst DL, Appelo CaJ. User's guide to PHREEQC version 3 — a computer program for speciation, batch-reaction, one-dimensional transport, and inverse geochemical calculations. U.S. Geological Survey techniques and methods 6; 2013. p. 519. [Chapter A43].

Perrin A-S, Probst A, Probst J-L. Impact of nitrogenous fertilizers on carbonate dissolution in small agricultural catchments: implications for weathering $CO_2$ uptake at regional and global scales. Geochim Cosmochim Acta 2008;72:3105–23. http://dx.doi.org/10.1016/j.gca.2008.04.011.

Purdy WC. A study of the pollution and natural purification of the Illinois River II. The plankton and related organisms. US Public Health Bull 1930:198.

Raich J, Tufekciogul A. Vegetation and soil respiration: correlations and controls. Biogeochemistry 2000;48:71–90. http://dx.doi.org/10.1023/A:1006112000616.

Raymond PA, Cole JJ. Increase in the export of alkalinity from North America's largest river. Science 2003;301:88–91. http://dx.doi.org/10.1126/science.1083788.

Raymond PA, Oh N-H. Long term changes of chemical weathering products in rivers heavily impacted from acid mine drainage: insights on the impact of coal mining on regional and global carbon and sulfur budgets. Earth Planet Sci Lett 2009;284:50–6. http://dx.doi.org/10.1016/j.epsl.2009.04.006.

Raymond PA, Oh NH, Turner RE, Broussard W. Anthropogenically enhanced fluxes of water and carbon from the Mississippi River. Nature 2008;451:449–52. http://dx.doi.org/10.1038/nature06505.

Reynolds RC, Johnson NM. Major element geochemistry of Lake Powell. In: Lake Powell Research Project Bulletin 5, editor. Institute for Geophysics and Planetary Physics. Los Angeles: University of California; 1974. p. 13.

Rice KC, Herman JS. Acidification of Earth: An assessment across mechanisms and scales. Applied Geochemistry 2012;27:1–14. http://dx.doi.org/10.1016/j.apgeochem.2011.09.001.

Runkel RL, Crawford CG, Cohn TA. Load estimator (LOADEST): a FORTRAN program for estimating constituent loads in streams and rivers. U.S. Geological Survey techniques and methods 4; 2004. p. 69. [Chapter A5].

Salisbury J, Green M, Hunt C, Campbell J. Coastal acidification by rivers: a threat to shellfish? EOS Trans Am Geophys Union 2008;89:513–4. http://dx.doi.org/10.1029/2008EO500001.

Schlesinger W, Andrews J. Soil respiration and the global carbon cycle. Biogeochemistry 2000;48:7–20. http://dx.doi.org/10.1023/A:1006247623877.

Smith SJ, van Aardenne J, Klimont Z, Andres RJ, Volke A, Delgado Arias S. Anthropogenic sulfur dioxide emissions: 1850–2005. Atmos Chem Phys 2011;11:1101–16.

Stets EG, Striegl RG. Carbon export by rivers draining the conterminous United States. Inland Waters 2012;2:177–84. http://dx.doi.org/10.5268/IW-2.4.510.

Stets EG, Kelly VJ, Broussard W, Smith TE, Crawford CG. Century-scale perspective on water quality in selected river basins of the conterminous United States. USGS scientific investigations report 2012-5225; 2012. p. 108.

Stoddard JL, Driscoll CT, Kahl JS, Kellogg JH. Can site-specific trends be extrapolated to a region? An acidification example for the Northeast. Ecol Appl 1998;8:288–99. http://dx.doi.org/10.1890/1051-0761(1998)008[0288:CSSTBE]2.0.CO;2.

Stoddard JL, Jeffries DS, Lukewille A, Clair TA, Dillon PJ, Driscoll CT, et al. Regional trends in aquatic recovery from acidification in North America and Europe. Nature 1999;401:575–8. http://dx.doi.org/10.1038/44114.

Van Breemen N, Mulder J, Driscoll CT. Acidification and alkalinization of soils. Plant and Soil 1983;75:283–308. http://dx.doi.org/10.1007/BF02369968.

Vernieu WS. Historical physical and chemical data for water in Lake Powell and from Glen Canyon Dam releases, Utah–Arizona, 1964–2012. US Geol Surv Data Ser 2013;471:32.

Vogl A, Lopes V. Impacts of water resources development on flow regimes in the Brazos River. Environ Monit Assess 2009;157:331–45. http://dx.doi.org/10.1007/s10661-008-0538-5.

White AF, Blum AE. Effects of climate on chemical weathering in watersheds. Geochim Cosmochim Acta 1995;59:1729–47. http://dx.doi.org/10.1016/0016-7037(95)00078-E.

Zeng F-W, Masiello CA, Hockaday WC. Controls on the origin and cycling of riverine dissolved inorganic carbon in the Brazos River, Texas. Biogeochemistry 2010;104:275–91. http://dx.doi.org/10.1007/s10533-010-9501-y.

Zhang YK, Schilling KE. Increasing streamflow and baseflow in Mississippi River since the 1940s: effect of land use change. J Hydrol 2006;324:412–22. http://dx.doi.org/10.1016/j.jhydrol.2005.09.033.